New Alfvén Continuum Gaps and Global Modes Induced by Toroidal Flow

B. van der Holst, A. J. C. Beliën, and J. P. Goedbloed

FOM-Institute for Plasma Physics, Association Euratom-FOM, P.O. Box 1207, 3430 BE Nieuwegein, The Netherlands

(Received 22 October 1999)

Continuous magnetohydrodynamic (MHD) spectra in tokamaks with toroidal rotation are studied. In the corotating frame, the linear perturbations experience Coriolis and centrifugal effects. The latter create Alfvén frequency gaps on rational surfaces resonant with the perturbations. New global eigenmodes are located inside these gaps. These modes may be used for MHD spectroscopy. In contrast to the usual gaps and toroidal Alfvén eigenmodes, the new flow-induced gaps and global modes are in the low frequency range so that they will have important implications for stability as well.

PACS numbers: 52.35.Bj, 52.30.–q, 52.55.Fa

Plasma flow is of extreme importance in the operation of present and future tokamaks, in particular, since fueling and exhaust considerations have to be taken into account. For example, divertor operation involves flow speeds in the scrape-off layer frequently exceeding the sound speed. On the other hand, shear flow can stabilize the pressure driven ballooning modes with a possibility for obtaining higher values of β (the ratio of kinetic to magnetic pressure) [1–3]. Shear flow can also suppress edge plasma turbulence and thereby create transport barriers. This facilitates improved high confinement operation [4].

In order to arrive at a complete picture of the global dynamics in tokamaks in the presence of flow, the complete spectrum of magnetohydrodynamic (MHD) waves and instabilities has to be computed in a genuine toroidal geometry, such as has been done in the past for static equilibria [5–7]. In the static case, it has been proven that the single frequencies of the continuous spectrum are determined by a system of ordinary differential equations in the poloidal angle on each flux surface. Continuous Alfvén and slow frequency bands are then obtained by varying the radial flux coordinate [8,9]. In cylinder geometry, global Alfvén eigenmodes may be found in the neighborhood of these continua [10,11]. In the toroidal case, gaps appear in the Alfvén continua due to avoided crossings of the cylindrical branches [12]. The gaps are important, since they create the conditions for the existence of global toroidal Alfvén eigenmodes (TAE) located inside these gaps [13]. These waves can be destabilized by fast α particles and therefore enhance transport [14]. Continuum damping [15,16] counteracts this effect. Comparing measured frequencies of these waves with computed ones can give valuable information about the plasma equilibrium. Such use of MHD waves for diagnostic purposes has been called MHD spectroscopy [17] and applied in the saddle coil experiments at JET [18,19].

In this Letter, we study the continua of tokamak equilibria with toroidal flow. New Alfvén gaps are found at low frequencies on rational surfaces resonant with the perturbations. These gaps are located at the $\Delta m = 0$ crossing of the cylindrical Alfvén continuum branches. For static equilibria, $\Delta m = 0$ gaps were also found [20,21], involving coupling of Alfvén and slow waves due to geodesic curvature and compressibility (or β) [8]. However, the new flow-induced $\Delta m = 0$ gaps do not depend on the latter effects, but are driven by centrifugal and Coriolis forces. Their width is significantly larger than the static $\Delta m = 0$ gaps. Moreover, a new global flow-induced mode is found that appears as one single mode inside these gaps, different from the beta-induced Alfvén eigenmodes (BAE) modes [21] which come in pairs in the static $\Delta m = 0$ gaps.

We consider a toroidally rotating axisymmetric tokamak with magnetic field $\mathbf{B} = \nabla\varphi \times \nabla\Psi + I(\Psi)\nabla\varphi$. Here, φ is the toroidal angle, $2\pi\Psi$ is the poloidal flux, and $I(\Psi) = RB_\varphi$, where R is the large radius and B_φ is the toroidal field. The plasma equilibrium satisfies force balance, $\nabla p = (\nabla \times \mathbf{B}) \times \mathbf{B} + \rho\Omega^2\mathbf{R}$, where $\mathbf{R} = R\mathbf{e}_R$ and $\Omega(\Psi)$ is the toroidal angular velocity. The last term of the force balance equation represents the outward pointing centrifugal force. The equilibrium can be solved by specifying an equation of state, like $\rho = \rho(\Psi)$ or $T = T(\Psi)$. Here, we use $\rho = \rho(\Psi)$ because of the demonstration of an unstable continuum. We also consider rigid rotations, since this facilitates the analysis. The numerical analysis is not restricted to these two assumptions, although the gap width and the gap mode frequency are different.

The linearized ideal MHD equations with equilibrium flow can be expressed by the force-operator formalism for the Lagrangian displacement $\boldsymbol{\xi}$ [22]. We make the normal mode ansatz $\boldsymbol{\xi} = \hat{\boldsymbol{\xi}} \exp i(n\varphi - \omega t)$. Using flux coordinates $(\Psi, \vartheta, \varphi)$ and exploiting a projection based on field lines and magnetic surfaces, modes localized around a particular magnetic surface are obtained by taking the limit of infinite normal gradient across that magnetic surface [8]. The normal component of $\boldsymbol{\xi}$ then becomes small so that the polarization of these modes is given by

$$\hat{\boldsymbol{\xi}} \approx g(\Psi - \Psi_0)\left[Y(\vartheta)\frac{1}{B^2}\,\mathbf{B} \times \nabla\Psi + Z(\vartheta)\mathbf{B} \right], \quad (1)$$

where the function g is δ-function-like and localized around Ψ_0. The frequencies $\tilde{\omega}(\Psi) = \omega - n\Omega(\Psi)$ in the locally corotating frame are determined by the eigenvalue equation

$$(-\rho\tilde{\omega}^2\mathsf{M} - 2\rho\tilde{\omega}\Omega\mathsf{C} + \mathsf{N} + \mathsf{G}) \cdot \begin{pmatrix} Y \\ Z \end{pmatrix} e^{in\varphi} = 0, \quad (2)$$

where

$$\mathsf{M} = \begin{pmatrix} \frac{R^2 B_p^2}{B^2} & 0 \\ 0 & B^2 \end{pmatrix}, \qquad \mathsf{C} = \begin{pmatrix} 0 & -i\mathbf{R}\cdot\mathbf{B} \\ i\mathbf{R}\cdot\mathbf{B} & 0 \end{pmatrix},$$

$$\mathsf{N} = \begin{pmatrix} F\,\frac{R^2 B_p^2}{B^2}\,F + \frac{\gamma p B^2}{\gamma p + B^2}\,\kappa_g^2 & -i\,\frac{\gamma p B^2}{\gamma p + B^2}\,\kappa_g F \\ iF\,\frac{\gamma p B^2}{\gamma p + B^2}\,\kappa_g & F\,\frac{\gamma p B^2}{\gamma p + B^2}\,F \end{pmatrix},$$

$$\mathsf{G} = \begin{pmatrix} -2\,\frac{I}{B^2}\,\kappa_g U + \frac{I^2}{B^2}\,V & iUF\,\frac{I}{B^2} + IV \\ -i\,\frac{I}{B^2}\,FU + IV & -i[FU] + B^2 V \end{pmatrix},$$

and the geodesic curvature, the parallel gradient operator, and the centrifugal terms are defined by

$$\kappa_g \equiv 2\,\frac{I}{JB^3}\,\frac{\partial B}{\partial\vartheta}, \qquad F \equiv -i\mathbf{B}\cdot\nabla, \qquad B_p = \frac{|\nabla\Psi|}{R}, \quad (3)$$

$$U \equiv \frac{B^2}{\gamma p + B^2}\,\rho\Omega^2\mathbf{R}\cdot\mathbf{B}, \quad (4)$$

$$V \equiv \frac{\rho}{B^2}\,\mathbf{B}\cdot\left[\Omega^2\mathbf{R}\left(\frac{1}{\rho}\,\nabla\rho - \frac{1}{\gamma p + B^2}\,\rho\Omega^2\mathbf{R}\right)\right]\cdot\mathbf{B}, \quad (5)$$

and the Jacobian $J = (\boldsymbol{\nabla}\Psi\times\boldsymbol{\nabla}\vartheta\cdot\boldsymbol{\nabla}\varphi)^{-1}$. The appropriate boundary conditions are poloidal periodicity of the Alfvén ($\sim Y$) and slow ($\sim Z$) eigenfunctions. Coupled Alfvén and slow continua are then obtained by varying the flux Ψ. In the corotating frame, the term linear in Ω represents the Coriolis effect and is denoted by the matrix C. Since the centrifugal force pierces flux surfaces obliquely, it strongly influences the continuous spectrum. The resulting terms appear in G and are analogous to gravitational contributions. Thus, the term in square brackets of V is a similar modification of the Brünt-Väisälä frequency as obtained for gravitational plasmas [23]. Equation (2) reduces to the eigenvalue equation studied in Ref. [24] for the special case of toroidal rotation in the absence of B_φ, where only G_{22} remains. An additional Eulerian continuum $n\Omega(\Psi)$ is found when starting from the Eulerian description. However, this continuum is decoupled from the Alfvén and slow continua.

In cylindrical geometry, the different poloidal harmonics $e^{im\vartheta}$ give separate Alfvén continua given by

$$\Omega_A^{\pm} = n\Omega \pm \frac{B_\varphi}{\sqrt{\rho}}\,\frac{1}{qR}\,(m + nq). \quad (6)$$

In toroidal geometry, these continua couple at the cylindrical crossover points $m + nq = -(m' + nq)$. Because of poloidal modulation of the equilibrium, toroidicity ($\Delta m = |m - m'| = 1$), ellipticity ($\Delta m = 2$), etc., induced gaps are formed there. (See, e.g., Refs. [12] and [25].) In the following, we investigate the lower frequency $\Delta m = 0$ Alfvén gaps.

As mentioned above, already for static equilibria $\Delta m = 0$ gaps are found in this frequency range. Figure 1 shows the continuous spectrum and gaps for a static equilibrium with circular cross section and inverse aspect ratio $\epsilon = a/R_0 = 0.1$. The safety factor increases monotonically from $q = 1.5$ on axis to $q = 2.89$ on the plasma edge. The rational surface $q = 2$ is located at $s \approx 0.8$. The Alfvén and slow continua are labeled according to their dominant polarization. Two peculiar gap features are visible: First, the $m = 2$ Alfvén continuum branches [originating far outside the frame at $\omega(s = 0) = \pm 0.34$] produce a gap ranging from $\mathrm{Re}(\omega) = -0.02$ to 0.02 associated with the rational surface. This gap is caused by the geodesic curvature term κ_g^2. Second, the $m = 1$ and $m' = 3$ slow continua couple at their crossover point, which is also located on the same rational surface. This coupling does not produce an ordinary $\Delta m = 2$ gap. Instead, the $m = 2$ Alfvén wave intervenes and pulls the continuum branch to $\omega = 0$ on this rational surface.

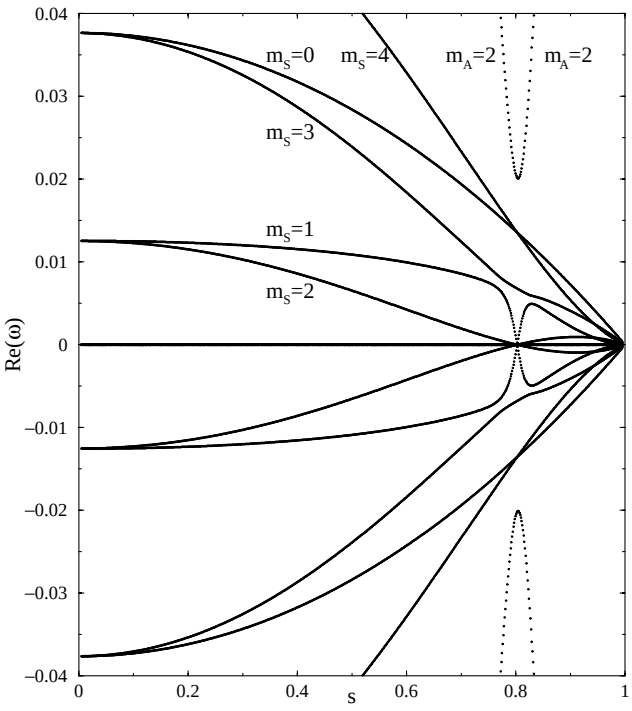

FIG. 1. Gap in the $m = 2$ Alfvén continuous spectrum at a rational and marginal $m + nq = 0$ surface and coupling of the $m = 1, 2, 3$ continua in that gap for a static equilibrium. The continua are plotted against $s = \sqrt{\Psi/\Psi_1}$. The main poloidal harmonic of the slow (m_s) and Alfvén (m_A) continua is indicated; $n = -1$, $\gamma = 5/3$, $\epsilon = 0.1$, $\beta = 0.049\%$, and $\rho(\Psi) \equiv 1$. The frequency ω is normalized as V_A/R_0.

The $\Delta m = 0$ gaps for static equilibria are caused by a subtle effect of the geodesic curvature and β. With flow, completely different $\Delta m = 0$ gaps found they are much wider, Doppler shifted, and much more robust. To demonstrate this, the Alfvén and slow continua are shown in Fig. 2(a) for a rigidly rotating equilibrium with $\Omega = 0.138 V_A/R_0$, where V_A is the Alfvén speed on axis. This corresponds to rather large flow speeds that may exceed the sound speed, representative for the situations discussed in the introduction. The safety factor increases monotonically from $q = 1.4$ on axis to $q = 2.46$ on the plasma edge. The rational surface $q = 2$ is located at $s \approx 0.89$. Since there is no poloidal flow, the density may be assumed to be a flux function (as discussed above): $\rho = 1 - 0.85 s^2$. Because of the flow, the continua are Doppler shifted and the symmetry with respect to the Doppler shifted frequency $n\Omega$ is broken through the Coriolis effect. In Fig. 2(a), the two $m = 2$ Alfvén continua produce a $\Delta m = 0$ gap at $s \approx 0.89$ ranging from $\mathrm{Re}(\omega) = -0.46$ to 0.19. Hence, due to the centrifugal forces, this gap is not only Doppler shifted but also becomes quite large.

In Fig. 2(b), the Alfvén part of the spectrum is highlighted by omitting the slow continua. The $\Delta m = 0$ Alfvén gap is thus clearly visible. Inside this gap a global eigenmode is found with a frequency $\mathrm{Re}(\omega) = -0.202$. For comparison, the gaps for the corresponding static case are shown in Fig. 2(c) (where the two symmetric BAE modes in the narrow $\Delta m = 0$ gap are omitted). The frequency of the flow-induced mode is in the same range as the slow continua. Therefore, resonant wave damping caused by the interaction of this global mode with the slow continua is almost unavoidable. Hence, the mode should be considered as a quasimode of the ideal MHD equations. This is demonstrated in the η convergence study of Fig. 3(a), similar to [26]. Two kinds of convergence studies are shown in one frame, viz., the convergence of the damping with respect to the plasma resistivity as $\eta \to 0$ and with respect to the number of radial grid points of the spectral code as $N_g \to \infty$. The frequency stays at $\mathrm{Re}(\omega) = -0.202$ and the damping converges to $\mathrm{Im}(\omega) \approx 7.5 \times 10^{-5}$. The damping to frequency ratio is 0.04%, i.e., quite small compared to the relative damping of ~5% obtained for TAE modes [16].

The asymmetric location of the flow-induced gap mode, shown in Fig. 2(b), demonstrates that the Coriolis effect is responsible. Otherwise, a symmetric partner should occur above the dashed line (in case of rigid rotation). Actually, at that location, global modes are found but they turn out to be resistive modes that disappear in the continuum in the

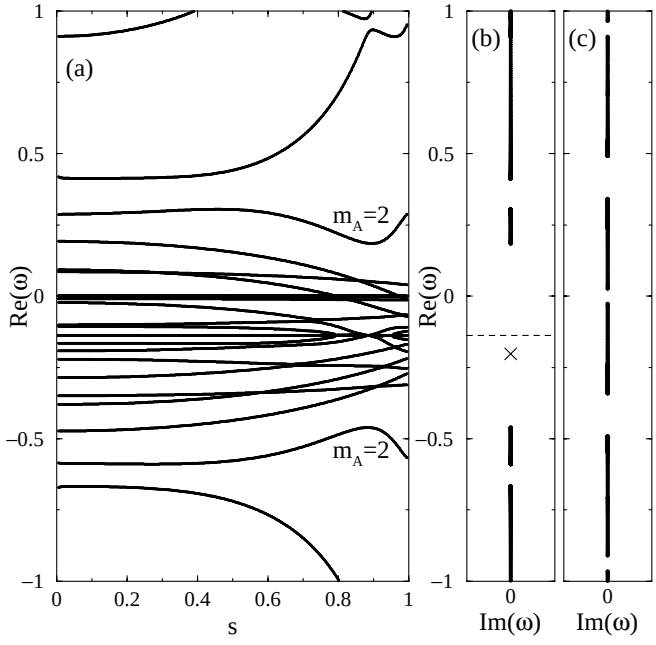

FIG. 2. Toroidal flow shifts the gap in the Alfvén continuum away from $\omega = 0$ and creates the conditions for a flow-induced global mode with frequency $\mathrm{Re}(\omega) = -0.202$: (a) Alfvén and slow continua plotted against s for $n = -1$ and $m = -1, \ldots, 5$. (b) The gap mode in the Alfvén spectrum is indicated by a cross and the Doppler shift $n\Omega$ by a dashed line; $\epsilon = 0.25$ and $\beta = 1\%$. (c) For a static equilibrium [$\Omega = 0$, but otherwise the same parameters as in 2(b)], the $\Delta m = 0$ gap around $\omega = 0$ is much smaller.

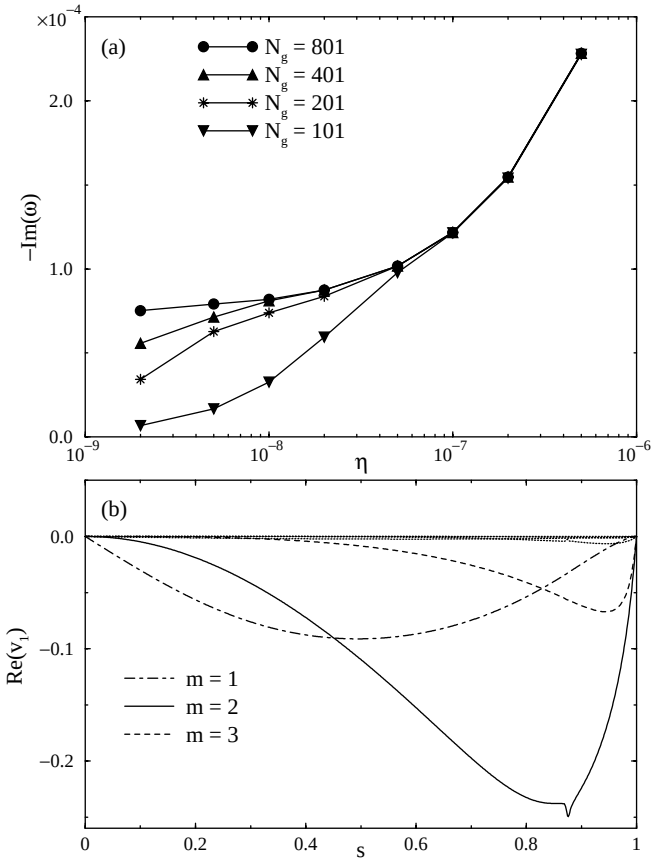

FIG. 3. (a) Continuum damping of the flow-induced global gap mode, and (b) modal content of the normal component of the perturbed velocity; $\eta = 5 \times 10^{-8}$, $N_g = 801$, and $m = -1, \ldots, 5$.

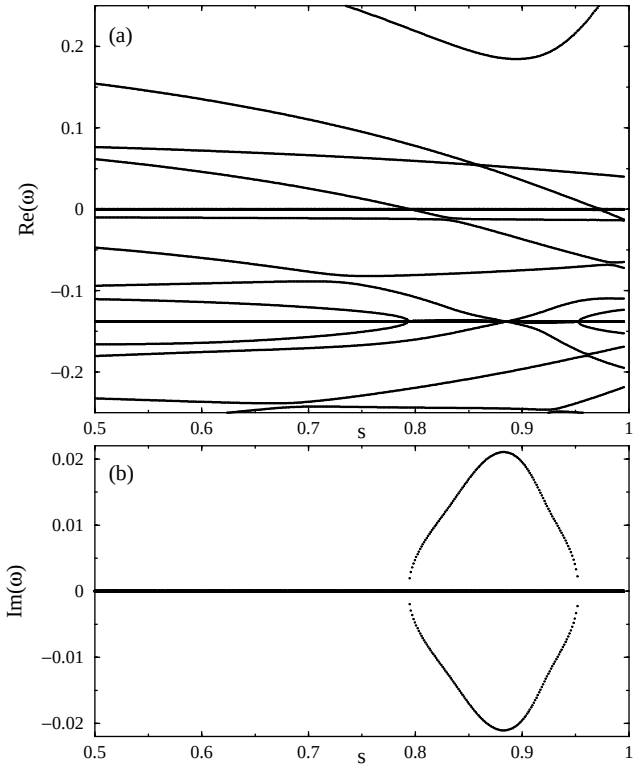

FIG. 4. (a) Blowup of the coalescence of two continuum branches in the $\Delta m = 0$ Alfvén gap of Fig. 2, and (b) the overstable continua at the merging frequencies.

limit $\eta = 0$. The asymmetric location of the flow-induced gap mode demonstrates that it is not a global Alfvén eigenmode (GAE) mode [10,11] (since it requires toroidicity) or a BAE mode [21] (since it does not require κ_g or β).

The modal content of the perturbed normal velocity component of the genuine gap mode is plotted in Fig. 3(b). This shows that the $m = 2$ harmonic is the dominant one and its maximum amplitude is located near the rational surface at $s \approx 0.89$, indicating that the mode has the same signature as the gap in which it is located. The near singular behavior at $s \approx 0.87$ due to the interaction with the continua is already visible in the normal velocity component, but it is more pronounced in the tangential components, which are not shown.

Possible destabilization of these waves by particles should be investigated. Since the frequencies of these waves are low, we do not expect that the excitation by fast α particles is important. However, the $\Delta m = 0$ gap and gap modes are in the same frequency domain as Doppler shifted instabilities. In our case, even the continua may be unstable. In Fig. 4(a) a blowup is shown of the continuum frequencies presented in Fig. 2(a). Two continuum branches merge at $s \approx 0.79$ and $s \approx 0.95$ and become overstable, as shown in Fig. 4(b). This unstable continuum is due to the entropy distribution along the field lines and it is analogous to convective instabilities of gravitational plasmas [24,27].

Summarizing, we have investigated the continuous MHD spectrum for tokamaks with toroidally rotating plasmas. In static equilibria, narrow Alfvén gaps appear on rational surfaces resonant with the linear perturbations. Toroidal flow creates wide gaps and global waves are found inside these gaps. The gaps are also important since they are in the low frequency region where instabilities originate so that they may give rise to new local instabilities (like ballooning) associated with the continuous spectra. Thus, these flow-induced gaps and gap modes are significant for the stability as well as the waves excited in MHD spectroscopy. In a forthcoming paper we will give a more detailed analysis of these results.

[1] A. Bhattacharjee *et al.*, Phys. Fluids B **1**, 2207 (1989).
[2] E. Hameiri and S. T. Chun, Phys. Rev. A **41**, 1186 (1990).
[3] F. L. Waelbroeck and L. Chen, Phys. Fluids B **3**, 601 (1991).
[4] R. J. Groebner, Phys. Fluids B **5**, 2343 (1993).
[5] R. Gruber *et al.*, Comput. Phys. Commun. **21**, 323 (1981).
[6] R. C. Grimm, R. L. Dewar, and J. Manickam, J. Comput. Phys. **49**, 94 (1983).
[7] W. Kerner *et al.*, J. Comput. Phys. **142**, 271 (1998).
[8] J. P. Goedbloed, Phys. Fluids **18**, 1258 (1975).
[9] Y. P. Pao, Nucl. Fusion **15**, 631 (1975).
[10] D. W. Ross, G. L. Chen, and S. M. Mahajan, Phys. Fluids **25**, 652 (1982); S. M. Mahajan, D. W. Ross, and G. L. Chen, Phys. Fluids **26**, 2195 (1983).
[11] K. Appert *et al.*, Plasma Phys. **24**, 1147 (1982); K. Appert, J. Vaclavik, and L. Villard, Phys. Fluids **27**, 432 (1984).
[12] C. E. Kieras and J. A. Tataronis, J. Plasma Phys. **28**, 395 (1982).
[13] C. Z. Cheng and M. S. Chance, Phys. Fluids **29**, 3695 (1986); C. Z. Cheng, L. Chen, and M. S. Chance, Ann. Phys. (N.Y.) **161**, 21 (1985).
[14] G. Y. Fu and J. W. van Dam, Phys. Fluids B **1**, 2404 (1989).
[15] H. L. Berk *et al.*, Phys. Fluids B **4**, 1806 (1992).
[16] S. Poedts *et al.*, Plasma Phys. Controlled Fusion **34**, 1397 (1992).
[17] J. P. Goedbloed *et al.*, Plasma Phys. Controlled Fusion **35**, B277 (1994).
[18] C. T. A. Huysmans *et al.*, Phys. Plasmas **2**, 1605 (1995).
[19] H. A. Holties *et al.*, Phys. Plasmas **4**, 709 (1997).
[20] M. S. Chu *et al.*, Phys. Fluids B **4**, 3713 (1992).
[21] A. D. Turnbull *et al.*, Phys. Fluids B **5**, 2546 (1993).
[22] E. Frieman and M. Rotenberg, Rev. Mod. Phys. **32**, 898 (1960).
[23] A. J. C. Beliën, S. Poedts, and J. P. Goedbloed, Astron. Astrophys. **322**, 995 (1997).
[24] T. A. K. Hellsten and G. O. Spies, Phys. Fluids **22**, 743 (1979).
[25] B. van der Holst *et al.*, Phys. Plasmas **6**, 1554 (1999).
[26] S. Poedts and W. Kerner, Phys. Rev. Lett. **66**, 2871 (1991).
[27] E. Hameiri, Phys. Fluids **26**, 230 (1983).